

What we learn from the learning rate

Rory A. Brittain,¹ Nick S. Jones,¹ and Thomas E. Ouldridge^{2,*}

¹*Department of Mathematics, Imperial College London, London, SW7 2AZ, UK*

²*Department of Bioengineering, Imperial College London, London, SW7 2AZ, UK*

The learning rate is an information-theoretical quantity for bipartite Markov chains describing two coupled subsystems. It is defined as the rate at which transitions in the downstream subsystem tend to increase the mutual information between the two subsystems, and is bounded by the dissipation arising from these transitions. Its physical interpretation, however, is unclear, although it has been used as a metric for the sensing performance of the downstream subsystem. In this paper we explore the behaviour of the learning rate for a number of simple model systems, establishing when and how its behaviour is distinct from the instantaneous mutual information between subsystems. In the simplest case, the two are almost equivalent. In more complex steady-state systems, the mutual information and the learning rate behave qualitatively distinctly, with the learning rate clearly now reflecting the rate at which the downstream system must update its information in response to changes in the upstream system. It is not clear whether this quantity is the most natural measure for sensor performance, and, indeed, we provide an example in which optimising the learning rate over a region of parameter space of the downstream system yields an apparently sub-optimal sensor.

I. INTRODUCTION

The mathematical theory of communication was founded by Claude Shannon in 1948 [1]. He was concerned with how to transfer a message from one point to another, and described the input signal through a random variable X and the output by a random variable Y . He introduced the Shannon entropy $H[X]$, which quantifies the *a priori* uncertainty in X ,

$$H[X] = - \sum_x p(x) \ln p(x), \quad (1)$$

where x labels the possible outcomes of the (discrete) random variable X . The logarithm can be taken with respect to any base; we choose to use natural logarithms, in which case entropy is measured in nats. If a meaningful signal is passed between X and Y , then knowledge of Y should reduce the uncertainty in X . The average uncertainty in X that remains given knowledge of Y is given by the conditional entropy

$$H[X|Y] = - \sum_{xy} p(x, y) \ln p(x|y), \quad (2)$$

where y labels the possible outcomes of Y . It is necessarily true that $H[X|Y] \leq H[X]$; it is not possible to become more uncertain about X by knowing Y [2]. The difference between the two quantities is the mutual information between X and Y [2],

$$I[X; Y] = H[X] - H[X|Y] = \sum_{xy} p(x, y) \log \frac{p(x, y)}{p(x)p(y)}. \quad (3)$$

The mutual information $I[X; Y]$ is symmetric with respect to switching X and Y .

The terminology “entropy” is suggestive of a link with thermodynamics. In fact, the entropy $H[X]$ is precisely the generalised non-equilibrium entropy of a thermodynamic system described by X [3–5]. Information is therefore indicative of a low entropy state, and recent work has focussed on the thermodynamic consequences of generating information [6–14], and the possibility of exploiting information to do useful work [15–19]. This body of work provides an explanation of Maxwell’s infamous demon [20] that does not rely on “erasure” of memories [20, 21]. The demon, by measuring its environment, appears to be able to extract work from equilibrium fluctuations. However, the demon can only extract work from its measurements if they generate non-equilibrium mutual information, and generating this mutual information in the first place requires consumption of thermodynamic resources [11, 13].

A key area in the interplay between information and thermodynamics is in biochemical sensing. Given that cells have a limited supply of resources, it is reasonable to ask whether these are put to optimally efficient use in sensing their environment — and if not, to explain why. Knowing the fundamental thermodynamic limits on sensor operation is also relevant to the engineering of synthetic sensors. Drawing on the connections between information and thermodynamics, several groups have considered the intrinsic costs associated with sensing and adaption (sensors that adapt revert to zero after lengthy exposure to a constant input) [12, 13, 22–31]. For example, Govern and Ten Wolde showed that molecular readout molecules of cell-surface receptors must consume free energy to form long-lived memories of receptor states [26, 27], a process equivalent to thermodynamic measurement of the kind performed by Maxwell’s demon [13]. Similarly, Bo, Del Giudice and Celani showed that the information stored by the molecular readouts about the entire trajectory of the receptors is bounded by the dissipation of the system minus the dissipation of the receptor transitions alone [12].

* t.ouldridge@imperial.ac.uk

A quantity, l_Y , called the learning rate has been proposed as a metric for the performance a sensor when the signal/sensor system is modelled as a bipartite Markov chain [32, 33]. The learning rate is bounded by the entropy production of the sensor so this appears to put an energetic bound on sensing quality. However, it is not clear that it is the most natural measure of sensing.

In this paper we will consider the behaviour of the learning rate for three simple steady-state systems, identifying and explaining differences between the physical content of l_Y and $I[X;Y]$. Typically, differences in behaviour arise because the learning rate quantifies the rate at which transitions in Y must act to restore information between X and Y , which is not necessarily closely related to the steady-state level of information or correlation. As a result, we are able to identify a fourth system in which optimizing over a parameter of the sensor at fixed input signal dynamics gives markedly different results when using the learning rate and the mutual information as metrics. In this case, optimising the mutual information provides the more intuitively reasonable optimal sensor.

II. SET UP: SENSING AND THERMODYNAMICS IN BIPARTITE MARKOV CHAINS

Bipartite Markov chains [9, 10] are a central tool in modelling Maxwell's demon-like behaviour and cellular sensing circuits. A bipartite Markov chain has states that are labelled with two variables x and y , which are generally taken to correspond to the states of two subsystems X and Y . Transitions only change one of the variables so the transition rate from (x, y) to (x', y') is

$$w_{yy'}^{xx'} = \begin{cases} w_y^{xx'} & \text{if } y = y' \text{ and } x \neq x', \\ w_{yy'}^x & \text{if } y \neq y' \text{ and } x = x', \\ 0 & \text{if } y \neq y' \text{ and } x \neq x'. \end{cases} \quad (4)$$

These rates have dimensions of inverse time. Throughout this paper we will use arbitrary units. The systems we will consider have a discrete state space and continuous time.

The second law of thermodynamics constrains the entropy production of the system to be positive. We can use the bipartite structure to separate the entropy production, \dot{S}_i , into six parts [9]

$$\dot{S}_i = d_t S^X + \dot{S}_r^X - \dot{I}^X + d_t S^Y + \dot{S}_r^Y - \dot{I}^Y \geq 0 \quad (5)$$

where the rates of increase of entropy of the X and Y subsystems are

$$\begin{aligned} d_t S^X &= \sum_{xx'} w_y^{xx'} p(x, y) \log \frac{p(x)}{p(x')}, \\ d_t S^Y &= \sum_{xyy'} w_{yy'}^x p(x, y) \log \frac{p(y)}{p(y')}, \end{aligned} \quad (6)$$

the rates of increase of the entropy of the environment due to transitions in X and Y are

$$\begin{aligned} \dot{S}_r^X &= \sum_{xx'} w_y^{xx'} p(x, y) \log \frac{w_y^{xx'}}{w_y^{x'x}}, \\ \dot{S}_r^Y &= \sum_{xyy'} w_{yy'}^x p(x, y) \log \frac{w_{yy'}^x}{w_{yy'}^y} \end{aligned} \quad (7)$$

and

$$\begin{aligned} \dot{I}^X &\equiv \sum_{xx'} w_y^{xx'} p(x, y) \log \frac{p(y|x')}{p(y|x)}, \\ \dot{I}^Y &\equiv \sum_{xyy'} w_{yy'}^x p(x, y) \log \frac{p(x|y')}{p(x|y)}. \end{aligned} \quad (8)$$

The flows \dot{I}^X and \dot{I}^Y are so called because they represent changes in the mutual information between X and Y due to transitions in X and Y respectively,

$$\frac{d}{dt} I[X;Y] = \dot{I}^X + \dot{I}^Y. \quad (9)$$

Importantly, the second law holds not just for Equation 5, but also for each subsystem individually [9, 32, 34]

$$\begin{aligned} d_t S^X + \dot{S}_r^X - \dot{I}^X &\geq 0, \\ d_t S^Y + \dot{S}_r^Y - \dot{I}^Y &\geq 0. \end{aligned} \quad (10)$$

This form of the second law has been extended by Horowitz [35] to systems with multiple subsystems that have independent noise, and has been used by Goldt and Seifert [36] to find the thermodynamic bound on the information learned by a feedforward neural network with Markovian dynamics.

We can identify $\sigma^X = d_t S^X + \dot{S}_r^X$ and $\sigma^Y = d_t S^Y + \dot{S}_r^Y$ as the the entropy productions of X and Y , ignoring the correlations between the two subsystems. $\dot{I}^Y < 0$ then allows for $\sigma^Y < 0$ — correlations between subsystems allow for apparent violation of the second law if the subsystems are erroneously considered in isolation. If $\sigma^Y < 0$ without direct energy flow from X to Y , X can be interpreted as a demon acting on subsystem Y . In terms of sensing, Y is generally interpreted as a sensory network for the signal X .

In steady state the mutual information is constant and so

$$\dot{I}^X + \dot{I}^Y = 0. \quad (11)$$

In this case, transitions in one subsystem must reduce the mutual information as much as the transitions in the other subsystem increase it.

The quantities \dot{I}^Y and \dot{I}^X have been introduced in Equation 5 to separate the second law into two parts. But since \dot{I}^Y represents the rate at which transitions in Y tend to increase information between X and Y , it has been named the learning rate $l_Y = \dot{I}^Y$ and proposed as a

metric for the performance of Y as a sensor of X [32, 33]. Identifying l_Y as a measure of sensory performance also sets a thermodynamic bound on sensor function, since from Equation 10, $l_Y \leq \sigma^Y$, the entropy generation due to transitions in Y . It is straightforward to show that one can equivalently write the learning rate as [33]

$$l_Y = \frac{d}{d\tau} I[X_t; Y_{t+\tau}] \Big|_{\tau=0}. \quad (12)$$

Intuitively, l_Y is the degree to which future values of Y are more predictive of the current value of X the current value of Y is, due to Y continuing to learn about X .

Although the use of the learning rate to quantify sensor performance seems reasonable from its definition, its physical interpretation has not been extensively explored. Other authors, such as Das *et al.* [31], have preferred the instantaneous mutual information, $I[X; Y]$, over l_Y as a metric for performance when deriving thermodynamic constraints on sensor function. Is l_Y essentially reporting the degree of interdependence between X and Y , similar to quantities like $I[X; Y]$ or the covariance $\text{Cov}(X, Y)$? Or does it highlight distinct features of the network? Is l_Y informative when trying to build optimal sensors for a given input signal? A further interpretational challenge occurs in steady state (a common setting for sensors). In this case [31–33]

$$l_Y = - \sum_{xyy'} w_{yy'}^x p(x, y) \log \frac{p(x, y)}{p(x, y')}, \quad (13)$$

and

$$l_Y = - \frac{d}{d\tau} I[X_{t+\tau}; Y_t] \Big|_{\tau=0}. \quad (14)$$

Equation 14 suggests that learning rate also reflects “nostalgia”, a quantity defined for discrete-time systems by Still *et al.* [8]. In steady state, l_Y not only reflects how much more the sensor Y learns about the current value of X as time progresses incrementally (Equation 12), but also the degree to which Y has nostalgic information about the history of X that is irrelevant to future signals (Equation 14). From this “nostalgia” perspective, it is unclear why large values of l_Y would correspond to effective sensing.

III. RESULTS AND DISCUSSION

A. The learning rate reports on correlations in the simplest bipartite sensing system

We first consider a canonical steady-state sensing system involving a two-state signal X and a two-state sensor Y , in which transitions propensities for X , $w_y^{xx'}$, are Y -independent [32, 37]. This 2×2 system is the simplest possible sensing setup. In biophysical terms, this system (illustrated in Figure 1) would correspond to a

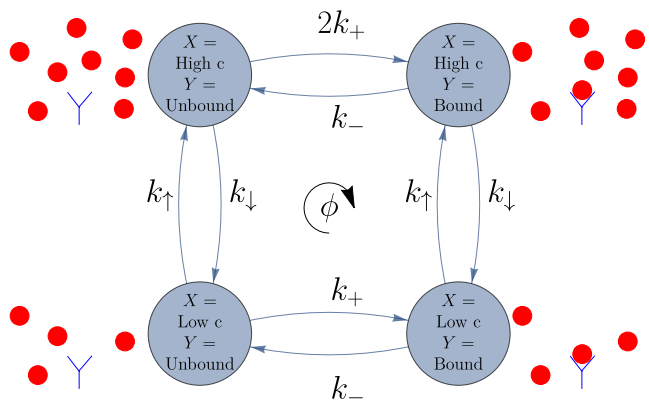


FIG. 1. The states and transitions for a simple system involving a two-state signal and a two-state sensor, in which the signal transitions are independent of the sensor state. We illustrate a biophysical interpretation of such a system, corresponding to an environment that can switch between high and low concentrations of ligand molecules, and a sensor that can bind to and unbind from the ligands. The rate of binding is proportional to the ligand concentration and the high concentration state has twice the concentration of the low concentration state in this illustration. The ligand concentration is absorbed into the transition rate k_+ . We illustrate the flux ϕ , the net flow of trajectories around the state space in steady state.

single receptor that can bind to ligand molecules, which is exposed to two discrete concentrations of ligands in its external environment [32]. The states $x = 0, 1$ correspond to low and high concentrations, and $y = 0, 1$ to unbound and bound receptors, respectively.

Let us, for convenience, assume that the high concentration is twice that of the low concentration. The rate at which the environment transitions from the low state to the high is k_+ and the reverse transition occurs at a rate k_- , independent of the receptor state. We only consider a single receptor molecule, which can be in two states: bound and unbound. The rate for a ligand molecule to bind to the receptor is proportional to the ligand concentration (i.e. mass-action kinetics and a well-mixed system are assumed). The concentrations are absorbed into the transition rates k_+ and $2k_+$ for ligand-binding in low and high concentration conditions, respectively. The rate of unbinding, k_- , is independent of the ligand concentration.

In Figure 2, we plot the instantaneous mutual information $I[X; Y]$, the learning rate l_Y and the covariance $\text{Cov}(X, Y)$ as a function of k_+ and k_- , at fixed k_+ and k_- (in this case, $k_+ = k_-$). Although the functions are not identical, the dependence on k_+ and k_- is very similar for all three. In particular, if $I[X; Y]$ is greater at (k_+, k_-) than at (k'_+, k'_-) then it is usually true that l_Y is greater at (k_+, k_-) than at (k'_+, k'_-) . The metrics are therefore almost equivalent for the purpose of optimising this sensor design. Deviations from this equivalence are manifest as non-parallel gradients of $I[X; Y]$ and l_Y with

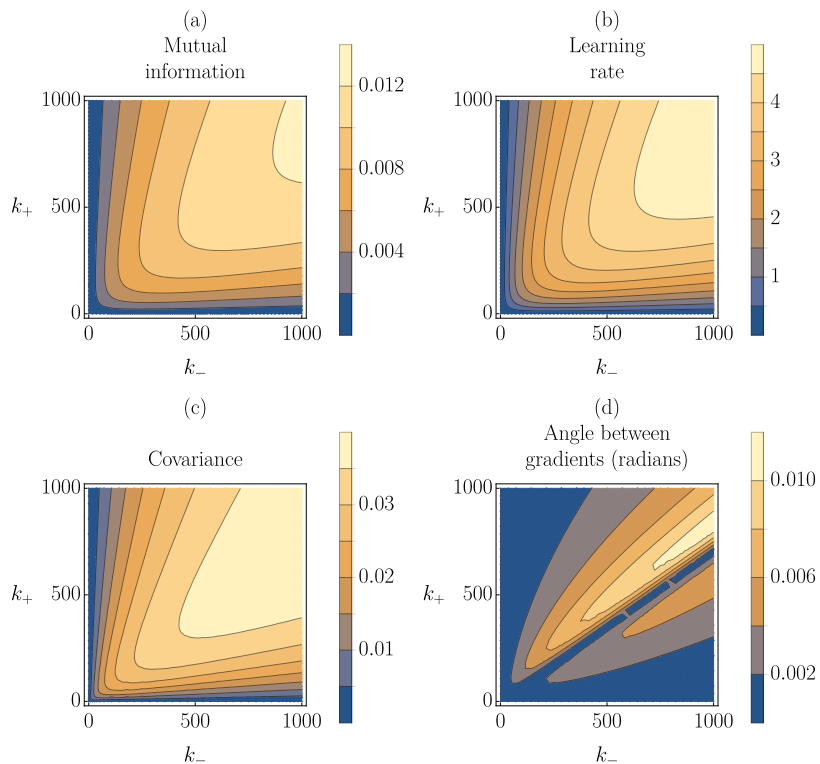


FIG. 2. The mutual information, learning rate and covariance all show similar behaviour as a function of sensor parameters for the simplest possible sensing device, illustrated in Figure 1. These quantities are plotted in (a), (b) and (c), respectively, as a function of k_+ and k_- , for $k_\uparrow = k_\downarrow = 100$. In (d), we plot the angle between $\nabla I[X; Y]$ and ∇l_Y , where ∇ is defined as differentiation with respect to (k_+, k_-) . The small angles observed suggest that there is little difference between optimizing for l_Y and for $I[X; Y]$.

respect to k_+ and k_- ; we plot the angle between gradients as a function of k_+ and k_- in Figure 2 (d), showing that it is small.

It is possible to understand this similarity from the underlying definition of the learning rate. Using the notation $p(x, y) = p_{xy}$, then Equation 13 can be expanded as

$$l_Y = - \left((w_{01}^0 p_{00} - w_{10}^0 p_{01}) \ln \frac{p_{00}}{p_{01}} \right) - \left((w_{10}^1 p_{10} - w_{01}^1 p_{11}) \ln \frac{p_{11}}{p_{10}} \right). \quad (15)$$

This simple system has one loop of states. In the steady state, any non-zero clockwise flux $\phi = w_{10}^0 p_{01} - w_{01}^0 p_{00}$ between the $(0, 1)$ and $(0, 0)$ states must be balanced by an equal clockwise flux for all other pairs of states around the loop, as illustrated in Figure 1. In particular, $\phi = w_{01}^1 p_{10} - w_{10}^1 p_{11}$ so

$$l_Y = \phi \ln \frac{p_{00} p_{11}}{p_{01} p_{10}}. \quad (16)$$

Clearly, the term within the logarithm in Equation 16 is related to the correlation between X and Y . If X and Y are more likely to be in the same state than different states then the logarithm is positive. If they are more

likely to be in different states then the log term is negative.

For this system the flux can be written

$$\begin{aligned} \phi &= p_{11} k_\downarrow - p_{01} k_\uparrow \\ &= p(Y=1|X=1)p(X=1)k_\downarrow \\ &\quad - p(Y=1|X=0)p(X=0)k_\uparrow. \end{aligned} \quad (17)$$

In this simple case we have assumed that X transitions are independent of Y , and thus $p(x)$ is determined solely by k_\uparrow and k_\downarrow : $p(X=1) = k_\uparrow / (k_\uparrow + k_\downarrow)$ and $p(X=0) = k_\downarrow / (k_\uparrow + k_\downarrow)$. Thus

$$\phi = \frac{k_\uparrow k_\downarrow}{k_\uparrow + k_\downarrow} \left(p(Y=1|X=1) - p(Y=1|X=0) \right). \quad (18)$$

The quotient in Equation 18 is independent of k_+ and k_- . It reflects the overall timescale of the process, which is manifest in the learning rate since l_Y is a dimensional quantity, and the uncertainty or entropy in X . The second part is clearly related, again, to the correlation between X and Y : it is large and positive when they are correlated, and large and negative when anticorrelated, just like the $\ln(p_{00} p_{11} / p_{01} p_{10})$ term in Equation 16.

Thus, for a 2×2 bipartite system, in which the value of Y does not influence the transitions in X , the learning

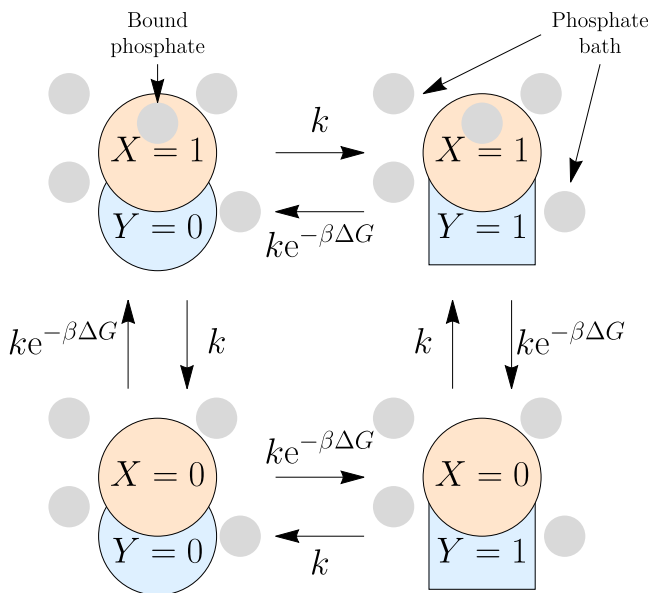


FIG. 3. A simple equilibrium molecular system, in which the X and Y represent the configurations of two proteins, X and Y . X can be phosphate-bound or unbound, and Y has two allosteric conformations. Relative rates of forwards and backwards transitions are set by overall free-energy differences.

rate l_Y essentially reports on the correlation between X and Y , and is thus closely related to the mutual information $I[X; Y]$ or covariance between X and Y . l_Y also incorporates a prefactor that reflects the overall timescale of the process. In Sections III B and III C, we shall violate the assumptions that lead to this conclusion and explore the consequences for the relationship between learning rate and mutual information.

B. Feedback from the downstream to the upstream system

The simplest way to violate the assumptions of Section III A is to allow the signal transition rates $w_y^{xx'}$ to depend on Y , whilst retaining the 2×2 structure of the overall system. To provide an intuition for such a setting, it is useful to consider the molecular system illustrated in Figure 3, containing two bound molecules, X and Y . Both molecules have two states; for concreteness, we imagine that X can be phosphorylated (bound to an inorganic phosphate moiety) or unphosphorylated, corresponding to states of a random variable $X = 1$ and $X = 0$, respectively. Molecule Y , by contrast, can adopt two allosteric conformations, and an energetic coupling between X and Y favours states $X, Y = 1, 1$ and $0, 0$ relative to $1, 0$ and $0, 1$.

If these molecules are in contact only with a bath of phosphate, they will eventually reach a thermodynamic equilibrium described by a Gibbs distribution. Assuming for simplicity that the free energies of the 11 and 00 states

are equal, and ΔG below the free energies of 10 and 01 ,

$$\begin{aligned} p_{10} &= p_{01} = \frac{e^{-\beta\Delta G}}{Z} \\ p_{00} &= p_{11} = \frac{1}{Z}, \end{aligned} \quad (19)$$

where $Z = 2 + 2e^{-\beta\Delta G}$ is the partition function, and β is the inverse temperature $1/k_B T$. At equilibrium, the system must obey detailed balance:

$$\frac{w_{01}^0}{w_{10}^0} = \frac{w_{10}^1}{w_{01}^1} = \frac{w_0^{01}}{w_0^{10}} = \frac{w_1^{10}}{w_1^{01}} = e^{-\beta\Delta G}. \quad (20)$$

The simplest choice consistent with this requirement is $w_{01}^0 = w_{10}^1 = w_0^{01} = w_1^{10} = k \exp(-\beta\Delta G)$; $w_{10}^0 = w_{01}^1 = w_0^{10} = w_1^{01} = k$.

The transitions in X are thus strongly influenced by the state of Y — a natural and necessary feature in an equilibrium system involving coupling between X and Y [27]. One can still evaluate Equation 13 in this setting, obtaining a nominal $l_Y = 0$ for all parameter choices. Indeed, l_Y is always zero in thermodynamic equilibrium; the contributions arising from each transition in Equation 13 must cancel with those arising from the reverse transitions. Similarly, Equation 16 still holds, but the flux ϕ is necessarily zero due to detailed balance, even though $I[X; Y]$ and $\text{Cov}(X, Y)$ can be large ($I[X; Y] = 0.56$ for $\beta\Delta G = 3.5$).

This equilibrium system and the driven system considered in Section III A are at opposite ends of a spectrum. In the equilibrium case, the influence of X on Y and Y on X are symmetric, in the sense that both experience the same biasing due to the interaction. Thus, there is no real sense in which Y is a sensor for X ; it causes changes in X as much as it reacts to them. For the driven system in Section III A, the influence is totally asymmetric; X influences Y but Y does not influence X at all, which is possible because the external process X is strongly driven. In this setting Y is a purely reactionary sensor.

One might argue that the “learning rate” is no longer a meaningful term for the quantity defined by the second line of Equation 8 in the setting where Y influences X . However, l_Y still quantifies the degree to which Y systematically reacts to (or learns about) X . To see this in more detail, we now take the unusual step of interpolating between the two limits of equilibrium and strong driving. We do this by adding a finite-strength non-equilibrium driving term to the equilibrium system, to explore the response of the learning rate.

This interpolation takes the form of additional transitions of rate q between X and X^* , independent of the state of molecule Y , alongside the original transitions of rate k and $k \exp(-\beta\Delta G)$. This system is illustrated in Figure 4 (a). We can vary q/k to interpolate between equilibrium ($q/k \rightarrow 0$) and strongly-driven ($q/k \rightarrow \infty$) systems; in the second case, X is independent of Y .

A possible way to implement this scheme in a molecular setting is to drive the system by allowing phosphorylation of X to occur by two additional pathways as

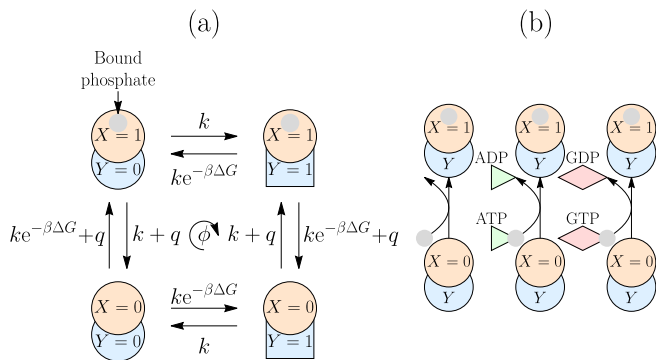
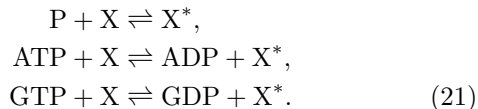


FIG. 4. (a) An extension of the system in Figure 3 in which it is possible to interpolate between the equilibrium limit and the limit where X is not influenced by Y by changing the ratio q/k . (b) This system could be implemented using three separate pathways for phosphorylation of X . The pathways are by binding phosphate from solution, or via donation of phosphate from ATP or ADP.

well as exchange of phosphate with solution. These additional pathways proceed via exchange of phosphate with nucleotides supplied by large buffers or chemostats, as shown in Figure 4 (b). With phosphate P and nucleotides ATP, ADP, GTP and GDP in solution, molecule X can change phosphorylation state by the following reactions



Here, X^* represents the molecule in the phosphorylated state. The concentrations of ATP, ADP, GTP and GDP contribute to the overall free energy changes of the second and third reactions; setting their concentrations to be incommensurate with the free energy change for $P + X \rightleftharpoons X^*$ amounts to driving the system so that it cannot reach equilibrium. For example, if $[\text{ADP}]$ and $[\text{GTP}]$ are both kept low, X will frequently be converted into X^* through interactions with ATP, but will be converted from X^* to X by interactions with GDP. The relative rate of these two reactions is not constrained by the relative rate of the two reactions involved in direct exchange of phosphate with solution, $P + X \rightleftharpoons X^*$, since the microscopic processes are distinct. Via this scheme it is therefore possible, at least in principle, to modify the stochastic process as shown in Figure 4 (a).

We perform this interpolation in Figure 5 (b), where we have plotted the mutual information and learning rate against q/k for $\beta\Delta G = 3.5$ at steady state. In this system the mutual information and learning rate behave quite differently. At $q/k = 0$, $I[X; Y]$ is large and its size is set by the energy gap; as $\beta\Delta G \rightarrow \infty$, $I[X; Y] \rightarrow \ln 2$, corresponding to perfect correlation. As q/k increases, X transitions start to become increasingly decoupled from the state of Y , and also much faster. Correlations are thus destroyed as shown in Figure 5 (a). The X state changes

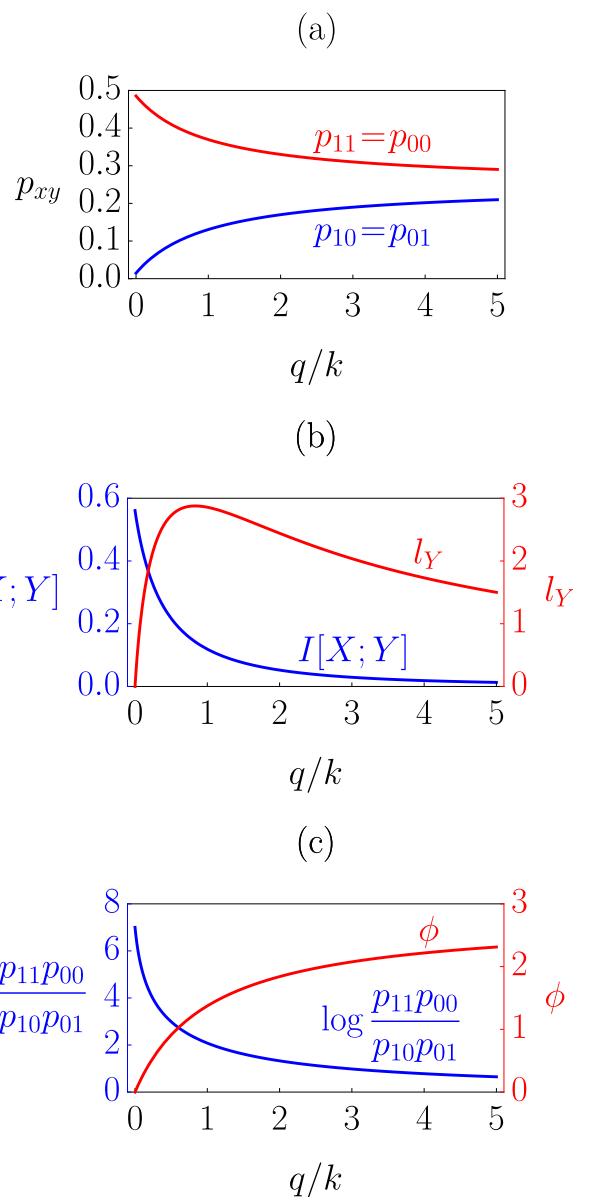


FIG. 5. The behaviour of a 2×2 system that interpolates between equilibrium and driven limits, illustrated in Figure 4(a). Plots obtained with $\beta\Delta G = 3.5$ and $k = 11.5$. (a) The non-equilibrium steady state probabilities. (b) The mutual information and learning rate behave distinctly. The learning rate is zero in the equilibrium limit ($q/k \rightarrow 0$) and then increases to a peak with increased driving q . The mutual information is highest at equilibrium and decreases as driving increases. (c) Two competing contributions to l_Y ; the flux ϕ and measure of correlation $\ln(p_{11}p_{00}/p_{10}p_{01})$, show opposite dependencies on q/k , leading to a peak at finite q/k .

randomly and too fast for Y to track it and consequently, $I[X; Y] \rightarrow 0$.

By contrast, the learning rate is zero for $q/k = 0$, has a peak at $q/k \sim 1$ and decays as $q/k \rightarrow \infty$. To understand this behaviour, it is helpful to consider Equation 16. For a 2×2 state system the learning rate is equal to the flux ϕ

around the states multiplied by a measure of the correlation between X and Y . As shown in Figure 5 (c), the measure of correlation $\ln(p_{11}p_{00}/p_{10}p_{01})$ behaves very similarly to $I[X; Y]$, but the flux ϕ increases with increased driving strength q/k . The result is the peaked shape of l_Y . Now that the assumption of no feedback from Y to X is violated, it is no longer true that ϕ and hence l_Y reflect the strength of correlation, as in Section III A.

What intuition, then, do we gain from the learning rate? The presence of a flux $\phi > 0$ is indicative of the fact that Y is responding to changes in X ; systematically, X tends to transition from 0 to 1 before Y , which then tends to follow. The dependence of l_Y on ϕ thus reflects the fact that the learning rate measures the degree to which transitions in Y respond to transitions in X to maintain correlations, rather than the strength of correlations themselves. This is apparent from the definitions in Equations 12 and 14. In a system with feedback from Y to X , these two metrics report on quite distinct properties. In the equilibrium limit, correlations are strong but transitions in Y are just as likely to precede transitions in X as to follow them, and hence the learning rate is zero.

C. A more complex signal process

In Section III B, we relaxed the assumption that the downstream system Y did not influence the upstream system X . As a result, the tight connection between learning rate and correlation between X and Y , observed in Section III A, was broken. We now explore the possibility of introducing more complex upstream signals X than assumed in Section III A, whilst restoring the assumption that X is not influenced by Y . We still consider systems in the stationary state.

As a physical model to provide intuition, we again consider a model of concentration sensing by a single receptor. In this case, we consider an oscillating concentration signal [38], as might be relevant to a cell experiencing roughly periodic, but noisy, fluctuations in its environment. Such a situation might be relevant to cells in animal intestines, for example. To construct an oscillating concentration, we consider a Markov process, X , with $2N$ discrete states, as shown in Figure 6 (a). States of X with $x = 1 \dots N$ have a concentration $C = xC_0/N$, and states $x = N + 1 \dots 2N$ have a concentration $C = (2N + 1 - x)C_0/N$. Thus there are N distinct concentrations, each present at two values of X . We consider transitions between only neighbouring X states, with $w^{xx+1} = Nk_\uparrow$ and $w^{xx-1} = Nk_\downarrow$.

This partitioning of X into two ‘‘rows’’ allows the construction of a Markov process X that leads to noisy oscillations in the concentration C , between $\frac{C_0}{N}$ and C_0 . Taking $Nk_\uparrow > Nk_\downarrow$, the system will tend to move to higher values of C when $1 \leq x \leq N$, and towards lower values when $N + 1 \leq x \leq 2N$ (clockwise in Figure 6 (a)). Scaling rate constants with N means that the overall

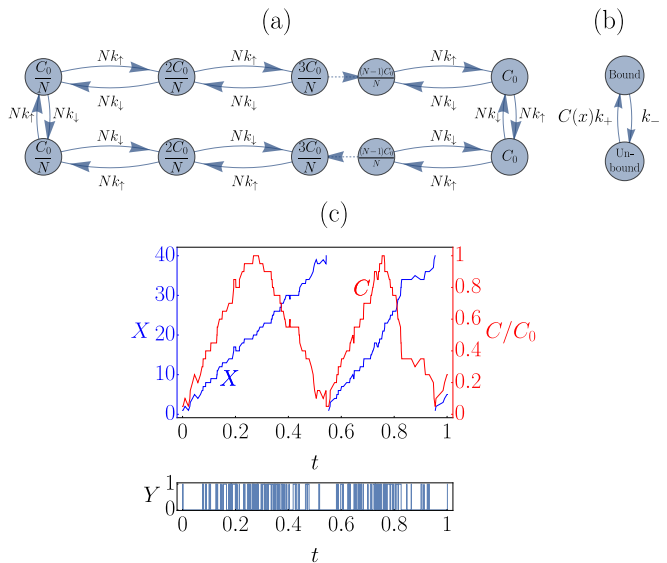


FIG. 6. A bipartite system in which a receptor modelled by Y responds to an oscillating concentration determined by X . (a) A graphical representation of the process X , indicating the ligand concentration C for each X . X is biased to move clockwise around the loop so C is driven up and then down in an oscillating fashion. X is not influenced by Y . (b) For Y , the binding rate is proportional to the ligand concentration and the unbinding rate is constant, as in Section III A. (c) Typical behaviour of X , C and Y over time (for $N = 20$, $C_0 = 1$, $k_\uparrow = 5$, $k_\downarrow = 0.5$ and $k_+ = k_- = 300$), showing stochastic oscillations in concentrations

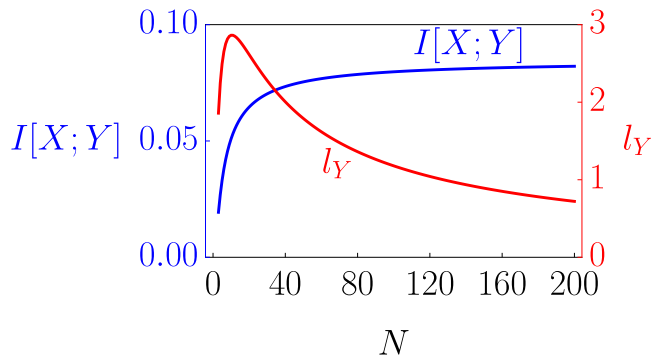


FIG. 7. The learning rate and instantaneous mutual information show opposite behaviours as the number of external states N is varied for the cyclic system illustrated in Figure 6 (a). The learning rate decays from a finite value to zero, whereas the instantaneous mutual information increases monotonically to a finite plateau. Data obtained for $k_\uparrow = 20$, $k_\downarrow = 10$, $k_+ = 10000$, $k_- = 2000$ and $C_0 = 1$.

flux around the cycle is N -independent. The typical behaviour of $X(t)$ and $C(t)$ is shown in Figure 6 (c). A similar Markov chain biased by a constant chemical potential to produce noisy oscillations was used by Barato and Seifert [39] to model a clock.

The receptor state defines the sub-process Y ; states

and transitions are shown in Figure 6 (b). The receptor properties are identical to that considered for the simpler system in Section III A. There is a constant rate of unbinding, $w_{10}^x = k_-$, and the binding rate $w_{01}^x = C(x)k_+$ is proportional to the ligand concentration.

From the perspective of the learning rate, it is illuminating to vary N (the number of discrete concentration states) whilst fixing all other parameters. As is evident from Figure 7, $I[X; Y]$ increases with N up to a finite plateau, whereas the learning rate decreases to zero. The behaviour of $I[X; Y]$ is intuitive; as more states are added, it becomes easier to reliably distinguish values of X that correspond to high and low values of C . In particular, for low N , C changes in large jumps due to X transitions, meaning that Y is an inaccurate reporter for X immediately after the transition. For larger N , the change in C is smoother. Eventually, however, this effect saturates, and $I[X; Y]$ reaches a finite plateau.

By contrast, the learning rate falls with N , tending to zero in the limit $N \rightarrow \infty$ (we present a general proof in Appendix A). To understand this difference in behaviour, note that our choice of $w^{xx+1} = Nk_\uparrow$ and $w^{xx-1} = Nk_\downarrow$ ensures that the overall average rate at which the concentration undergoes oscillations is fixed, regardless of N . The number of forward and backward steps of the process X in a time Δt are independently Poisson-distributed with means $Nk_\uparrow\Delta t$ and $Nk_\downarrow\Delta t$, respectively. Thus the mean net number of forward steps in Δt is $\Delta tN(k_\uparrow - k_\downarrow)$, proportional to N , compensating for the fact there are more states covering the same concentration window. The standard deviation in the net number of forward steps in Δt is $\sqrt{\Delta tN(k_\uparrow + k_\downarrow)}$, however. Consequently, as N is increased, the relative uncertainty in the net number of forward steps during Δt falls as $1/\sqrt{N}$. Larger N therefore implies a smaller relative error in predicting the future value of X , given knowledge of its current value. Increasing the number of states N is thus effectively a method to interpolate between highly stochastic and quasi-deterministic behaviour of X . Note that it is the convergence on deterministic behaviour of the signal that in general takes $l_Y \rightarrow 0$; not $N \rightarrow \infty$.

As $N \rightarrow \infty$, therefore, the rate at which the current value of Y becomes ineffective in predicting future values of X tends towards zero. In other words, the “nostalgia” of Y (Equation 14 and Ref. [8]), and hence l_Y , tends towards zero. The learning rate quantifies the rate at which transitions in Y must respond to transitions in X to maintain a steady-state information; this rate is zero for large N despite $I[X; Y]$ increasing monotonically with N . Thus, using a more complex signal than in the simple 2×2 network in Section III A also serves to highlight the distinctions between the physical meaning of l_Y and $I[X; Y]$.

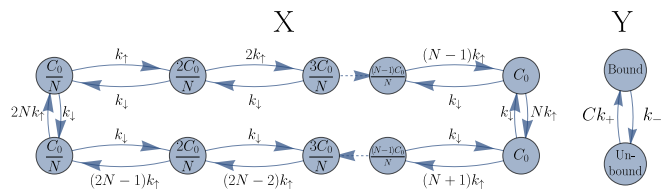


FIG. 8. A bipartite system X, Y for which optimising the parameters of the downstream subsystem Y to maximise learning rate and mutual information give markedly different results. The system is essentially identical to that considered in Figure 6, but with hopping rates for the upstream process X that depend on x .

D. Optimisation of sensors

Due to its provenance as an informational quantity, l_Y has been proposed as a metric for sensor performance in steady-state sensing circuits [32, 33]. In Sections III B and III C, however, we have emphasised that l_Y reflects the rate at which transitions in the downstream subsystem Y respond to changes in X to maintain a steady-state information $I[X; Y]$. There is no reason *a priori* to suppose that maximising such a quantity is inherently optimal for a sensor — indeed, one might imagine that having to compensate for transitions in X at a lower rate would be preferable in reliable sensing. Further, our results in Sections III B and III C show that the response of l_Y to parameter variation can be unrepresentative of the degree to which Y relates to signal X .

Sections III B and III C, however, cannot reasonably be described as sensor optimisation. To optimise a sensor, it is natural to consider a setting in which the dynamics of signal X are fixed, and optimisation is performed over the parameters of the downstream network Y . In Sections III B and III C, however, we considered the response of l_Y to variations in the dynamics of X . Moreover, in Section III B, we even considered a “downstream” network Y which influences the “upstream” network X . This is hardly a well-defined sensor. In the simple system of Section III A, for which we did consider variation over the parameters of the Y sub-process, and X was not influenced by Y , optimising l_Y and $I[X; Y]$ over sensor parameters was essentially equivalent. It is therefore worth considering whether signal/sensor architectures do exist in which optimising over the sensor parameters for l_Y and $I[X; Y]$ give markedly different results.

To demonstrate this possibility, we consider a system identical to the oscillating concentration sensor considered in Section III C, but for which the transition rates of the X sub-process are x -dependent (Figure 8). The sensor Y , with transition rates $w_{10}^x = k_-$ and $w_{01}^x = C(x)k_+$, is unchanged.

We consider optimising over the relative rates of the X and Y subsystems at fixed number of X states N , fixed transition rates in the X subsystem, and fixed k_+/k_- within Y . In Figure 9, we show that the instanta-

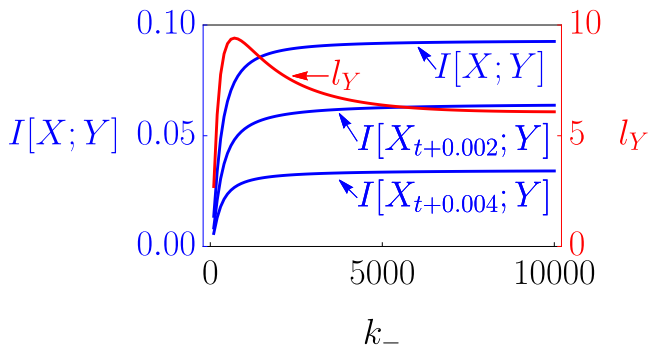


FIG. 9. For a sensor detecting an oscillating system with a non-uniform hopping rate, $I[X; Y]$ increases monotonically with the relative response rate of the sensor, whereas l_Y shows a peak at a finite response rate. The two metrics thus imply distinct “optimal” sensors. Also shown are some examples of $I[X_{t+\tau}; Y_t]$, where τ is a positive time delay. These too are monotonic in response rate. Data obtained for $N = 20$, $k_{\uparrow} = 200$, $k_{\downarrow} = 10$, $k_{+}/k_{-} = 2$ and $C_0 = 1$

neous mutual information increases monotonically with the rates of the downstream subsystem (represented by k_{-}), from $I[X; Y] = 0$ up to a plateau. By contrast, the learning rate increases from $l_Y = 0$ to a peak at finite k_{-} , before decaying to a plateau. Maximising the instantaneous mutual information and maximising the learning rate give qualitatively different “optimal sensors”.

We have considered optimising over this subspace with k_{+}/k_{-} fixed rather than the whole (k_{+}, k_{-}) space for ease of illustration. For a metric to be useful for sensor optimisation it must be able to meaningfully differentiate sensing quality between any two sets of parameters, and provide a useful optimisation within any subspace of the parameter space. We note that similar behaviour is observed for other values of k_{+}/k_{-} .

The “optimal sensor” indicated by the instantaneous mutual information is intuitively reasonable. When the rates of the sensor are as large as possible, Y can keep up with X ; otherwise it simply lags behind, reporting earlier values of X . Whilst it is possible that a slower-responding sensor could provide lower $I[X, Y]$, but increased predictive power at some specific future time τ , $I[X_{t+\tau}; Y_t]$ [38], we find no evidence of this for our case (see Figure 9). Therefore the instantaneous mutual information provides a metric for sensor performance that is intuitively reasonable, if not necessarily unique. By contrast, we can find no intuitive justification of the peak of the learning rate in terms of optimal sensing. Indeed, the peak in the learning rate is reminiscent of the peak in the dissipation rate σ_Y that arises in such systems [40]. This peak is indicative of a subsystem Y that lags behind X sufficiently that the response to driving is highly irreversible, but is not so slow that it barely responds at all [40]. Similarly, it is plausible that the peak in l_Y reflects a delay in Y relative to X that is large enough to ensure that transitions have a strong tendency to increase $I[X; Y]$, but not

so large that Y barely responds to changes in X at all. Regardless, since we are unable to explain the location of this peak through any optimal tracking perspective, it is difficult to see how l_Y is informative of quality of sensing.

IV. CONCLUSIONS

We have explored the physical interpretation of the learning rate l_Y , a recently proposed statistical metric defined on bipartite stochastic systems [32, 33, 41]. l_Y quantifies the rate at which transitions in a downstream system Y act to increase the mutual information between Y and an upstream system X , or the rate at which future values of Y become more predictive of the current values of X than the current value of Y . In the steady state, a biophysically relevant scenario, l_Y is also equivalent to the rate at which transitions in X reduce the mutual information, or the “nostalgia” rate at which information about the current value of X becomes irrelevant.

We have shown that, in the simplest steady-state bipartite system in which X is not influenced by Y , l_Y essentially reports on the correlation between subsystems. In other settings l_Y can show quantitatively and qualitatively different behaviour from measures of interdependence such as the mutual information and covariance. Moreover, we have demonstrated that this difference can be explained by the fact that l_Y quantifies the rate at which transitions in Y act to maintain a steady state $I[X; Y]$, rather than the magnitude of $I[X; Y]$. In general, there is no reason why these two properties should behave similarly.

The “learning rate” is thus a good description of the quantity l_Y , but despite this we do not find that l_Y is a good general metric for sensor performance, as has been proposed [32, 33]. A sensor that needs to consistently learn at a high rate is not obviously optimal — indeed, it would seem better to store information about the current value of the signal that does not quickly become irrelevant. We have shown that, in at least one signal/sensor context, maximising the learning rate over a subset of sensor parameters gives a result which is hard to interpret as an optimal sensor. Without first identifying how the learning rate is reporting on sensor performance in a given context, it is difficult to see how l_Y can be reliably used as a metric for sensing in general.

Our work has considered only a small set of possible Markovian systems, and has not touched on issues such as performance of readout networks that are designed to integrate a signal over time [13, 26] or perform more complex operations such as differentiation [38]. It is possible that the learning rate reflects an aspect of the performance in these circuits. Further, we have not investigated the behaviour of the learning rate in systems that are yet to reach steady state. In such cases, l_Y is no longer equal to either the nostalgia rate, or the rate at which transitions in X tend to reduce $I[X; Y]$. Moreover, it is potentially non-zero even for passive (non-driven)

systems. The meaning of the learning rate in such cases warrants further consideration.

Finally, the learning rate can provide insight into the functioning of systems even if it is not a metric for performance of sensing or similar functionality. For example, its properties were recently applied to derive results that do not depend on its interpretation in a simple model of a perceptron [36]. l_Y can also reasonably be interpreted as an indicator of the direction and magnitude of information flow in a steady-state bipartite network, as evidenced by its role in the refined second law (Equation 10). One interpretation of the learning rate in steady state might be as a quantification of how hard the downstream system has to work to maintain a certain interdependence of X and Y , regardless of whether this interdependence is optimal in some sense. Indeed, l_Y is bounded from above by σ_Y , the thermodynamic entropy production rate due to transitions in the Y subsystem. It should be noted, however, that although entropy is generated by Y transitions, this is not necessarily indicative of a consumption of resources held by the Y subsystem [32]. In the biomolecular examples given here, for exam-

ple, the Y subsystems are totally passive, consuming no chemical fuel [27]. The thermodynamic work is done by the driving of the external process X [32], which is particularly evident in the example of Section III B, where the nucleotides fueling the driving are explicitly considered. From the perspective of a sensor or a cell, entropy generation arising from environmental changes, rather than due to internal fuel consumption, is not obviously a limiting factor.

V. ACKNOWLEDGEMENTS

We acknowledge Susanne Still for a discussion of the topics and Pieter Rein ten Wolde, Andre Barato, Udo Seifert, David Hartich and Sebastian Goldt for commenting on the manuscript.

T. E. O. acknowledges support from a Royal Society University Research Fellowship and R. A. B. acknowledges support from an Imperial College London AMMP studentship.

-
- [1] Shannon C E, *A mathematical theory of communication*, 1948 *Bell Syst. Tech. J.* **27**(3) 379–423
 - [2] Cover T M and Thomas J A, *Elements of Information Theory*, Wiley-Interscience 2006
 - [3] Crooks G E, *Entropy production fluctuation theorem and the nonequilibrium work relation for free energy differences*, 1999 *Phys. Rev. E* **60** 2721–2726
 - [4] Jarzynski C, *Equalities and inequalities: Irreversibility and the second law of thermodynamics at the nanoscale*, 2011 *Annu. Rev. Condens. Matter Phys.* **2** 329–351
 - [5] Seifert U, *Stochastic thermodynamics, fluctuation theorems and molecular machines*, 2012 *Rep. Prog. Phys.* **75** 126001
 - [6] Sagawa T and Ueda M, *Minimal energy cost for thermodynamic information processing: Measurement and information erasure*, 2009 *Phys. Rev. Lett.* **102** 250602
 - [7] Sagawa T and Ueda M, *Fluctuation theorem with information exchange: Role of correlations in stochastic thermodynamics*, 2012 *Phys. Rev. Lett.* **109** 180602
 - [8] Still S, Sivak D A, Bell A J, and Crooks G E, *Thermodynamics of prediction*, 2012 *Phys. Rev. Lett.* **109** 120604
 - [9] Horowitz J M and Esposito M, *Thermodynamics with continuous information flow*, 2014 *Phys. Rev. X* **4** 031015
 - [10] Hartich D, Barato A C, and Seifert U, *Stochastic thermodynamics of bipartite systems: Transfer entropy inequalities and a Maxwell’s demon interpretation*, 2014 *J. Stat. Mech.* **2014**(2) P02016
 - [11] Parrondo J M R, Horowitz J M, and Sagawa T, *Thermodynamics of information*, *Nat. Phys.* **11**(2) 131–139
 - [12] Bo S, Del Giudice M, and Celani A, *Thermodynamic limits to information harvesting by sensory systems*, 2015 *J. Stat. Mech.* **2015**(1) P01014
 - [13] Ouldridge T E, Govern C C, and ten Wolde P R, *The thermodynamics of computational copying in biochemical systems*, arXiv:1503.00909 [cond-mat.stat-mech]
 - [14] Ouldridge T E and ten Wolde P R, *Fundamental costs in the production and destruction of persistent polymer copies*, arXiv:1609.05554 [cond-mat.stat-mech]
 - [15] Bauer M, Abreu D, and Seifert U, *Efficiency of a Brownian information machine*, 2012 *J. Phys. A: Math. Theor.* **45** 162001
 - [16] Horowitz J M, Sagawa T, and Parrondo J M R, *Imitating chemical motors with optimal information motors*, 2013 *Phys. Rev. Lett.* **111** 010602
 - [17] Chapman A and Miyake A, *How an autonomous quantum Maxwell demon can harness correlated information*, 2015 *Phys. Rev. E* **92** 062125
 - [18] McGrath T, Jones N S, ten Wolde P R, and Ouldridge T E, *Biochemical machines for the interconversion of mutual information and work*, 2017 *Phys. Rev. Lett.* **118** 028101
 - [19] Yamamoto S, Ito S, Shiraishi N, and Sagawa T, *Linear irreversible thermodynamics and Onsager reciprocity for information-driven engines*, 2016 *Phys. Rev. E* **94** 052121
 - [20] Bennett C H, *Notes on Landauer’s principle, reversible computation, and Maxwell’s demon*, 2003 *Stud. Hist. Philos. M. P.* **34** 501–510
 - [21] Landauer R, *Irreversibility and heat generation in the computing process*, 1961 *IBM J. Res. Dev.* **5** 183–191
 - [22] Tu Y, *The nonequilibrium mechanism for ultrasensitivity in a biological switch: Sensing by Maxwell’s demons*, 2008 *Proc. Nat. Acad. Sci. USA* **105** 11737–11741
 - [23] Lan G, Sartori P, Neumann S, Sourjik V, and Tu Y, *The energy-speed-accuracy trade-off in sensory adaptation*, 2012 *Nat. Phys.* **8** 422–428
 - [24] Sartori P, Granger L, Lee C F, and Horowitz J M, *Thermodynamic costs of information processing in sensory adaptation*, 12 2014 *PLoS Comput. Biol.* **10**(12) 1–9
 - [25] Mehta P and Schwab D J, *Energetic costs of cellular computation*, 2012 *PNAS* **109**(44) 17978–17982

- [26] Govern C C and ten Wolde P R, *Optimal resource allocation in cellular sensing systems*, 2014 *Proc. Nat. Acad. Sci. USA* **111** 17486–17491
- [27] Govern C C and ten Wolde P R, *Energy dissipation and noise correlations in biochemical sensing*, 2014 *Phys. Rev. Lett.* **113** 258102
- [28] ten Wolde P R, Becker N B, Ouldrige T E, and Mugler A, *Fundamental limits to cellular sensing*, 2016 *J. Stat. Phys.* **162**(5) 1395–1424
- [29] Mancini F, Marsili M, and Walczak A M, *Trade-offs in delayed information transmission in biochemical networks*, 2016 *J. Stat. Phys.* **162**(5) 1088–1129
- [30] Ito S and Sagawa T, *Maxwell's demon in biochemical signal transduction with feedback loop*, 2015 *Nat. Commun.* **6** 7498
- [31] Das S G, Rao M, and Iyengar G, *A lower bound on the free energy cost of molecular measurements*, arXiv:1608.07663 [cond-mat.stat-mech]
- [32] Barato A C, Hartich D, and Seifert U, *Efficiency of cellular information processing*, 2014 *New J. Phys.* **16**(10) 103024
- [33] Hartich D, Barato A C, and Seifert U, *Sensory capacity: An information theoretical measure of the performance of a sensor*, 2016 *Phys. Rev. E* **93** 022116
- [34] Allahverdyan A E, Janzing D, and Mahler G, *Thermodynamic efficiency of information and heat flow*, 2009 *J. Stat. Mech.* **2009**(09) P09011
- [35] Horowitz J M, *Multipartite information flow for multiple Maxwell demons*, 2015 *J. Stat. Mech.* **2015**(3) P03006
- [36] Goldt S and Seifert U, *Stochastic thermodynamics of learning*, Jan 2017 *Phys. Rev. Lett.* **118** 010601
- [37] Barato A C, Hartich D, and Seifert U, *Information-theoretic versus thermodynamic entropy production in autonomous sensory networks*, 2013 *Phys. Rev. E* **87**(4) 042104
- [38] Becker N B, Mugler A, and ten Wolde P R, *Optimal prediction by cellular signaling networks*, 2015 *Phys. Rev. Lett.* **115** 258103
- [39] Barato A C and Seifert U, *Cost and precision of Brownian clocks*, 2016 *Phys. Rev. X* **6** 041053
- [40] Becker N B, Mugler A, and ten Wolde P R, *Prediction and dissipation in biochemical sensing*, 2013 arXiv:1312.5625 [q-bio.MN]
- [41] Zhang Y and Barato A C, *Critical behavior of entropy production and learning rate: Ising model with an oscillating field*, 2016 *J. Stat. Mech.* **2016**(11) 113207

Appendix A: Proof that l_Y tends to zero as $N \rightarrow \infty$ for the system in Section III C

Using Equations 8 and 11, in the steady state

$$l_Y = -\dot{I}^X = -\sum_{xx'y} w^{xx'} p(x, y) \log \frac{p(y|x')}{p(y|x)} = \sum_{xx'y} w^{xx'} p(x, y) (\log p(y|x) - \log p(y|x')).$$

Relabelling dummy variables,

$$l_Y = \sum_{xx'y} \left(p(x, y) w^{xx'} - p(x', y) w^{x'x} \right) \log p(y|x). \quad (\text{A1})$$

In this system, $p(x) = \frac{1}{2N}$ for all x by symmetry. There are only transitions between adjacent X states and so

$$l_Y(N) = \frac{1}{2N} \sum_{xy} \left(p_N(y|x) w^{xx^+} - p_N(y|x^+) w^{x^+x} + p_N(y|x) w^{xx^-} - p_N(y|x^-) w^{x^-x} \right) \log p_N(y|x) \quad (\text{A2})$$

where x^+ is the next X state in the cycle and x^- is the previous state, and we have introduced an explicit dependence of probabilities on N . In this system

$$\begin{aligned} w^{xx^+} &= w^{x^-x} = Nk_{\uparrow}, \\ w^{x^+x} &= w^{xx^-} = Nk_{\downarrow}, \end{aligned} \quad (\text{A3})$$

and therefore

$$l_Y(N) = \frac{1}{2} \sum_{xy} \left(k_{\uparrow} (p_N(y|x) - p_N(y|x^-)) + k_{\downarrow} (p_N(y|x) - p_N(y|x^+)) \right) \log p_N(y|x). \quad (\text{A4})$$

Defining $z = \frac{x}{2N}$ we have

$$l_Y = \frac{1}{2} \sum_{zy} \left(k_{\uparrow} (p_N(y|z) - p_N(y|z - \frac{1}{2N})) + k_{\downarrow} (p_N(y|z) - p_N(y|z + \frac{1}{2N})) \right) \log p_N(y|z). \quad (\text{A5})$$

We now assume that for large N , $p_N(y|z)$ tends smoothly towards $p_\infty(y|z)$, where $p_\infty(y|z)$ is a smooth function of z with $p_\infty(y|0) = p_\infty(y|1)$ due to the boundary conditions that connect $z = 1$ ($x = 2N$) to $z = 0$ ($x = 0$). For sufficiently large N ,

$$p_N(y|z) = p_\infty(y|z) + \frac{1}{N} \left. \frac{dp_N(y|z)}{d1/N} \right|_{N \rightarrow \infty} + \mathcal{O}\left(\frac{1}{N^2}\right). \quad (\text{A6})$$

Thus

$$p_N(y|z \pm \frac{1}{2N}) = p_\infty(y|z) \pm \frac{1}{2N} \frac{dp_\infty(y|z)}{dz} + \frac{1}{N} \left. \frac{dp_N(y|z)}{d1/N} \right|_{N \rightarrow \infty} + \mathcal{O}\left(\frac{1}{N^2}\right)$$

and the sum can be approximated by an integral

$$\sum_z \frac{1}{2N} f(z) \rightarrow \int_0^1 dz f(z) + \mathcal{O}\left(\frac{1}{N}\right). \quad (\text{A7})$$

So for large N ,

$$l_Y(N) = \frac{1}{2} \sum_y \int_0^1 dz \left((k_\uparrow - k_\downarrow) \frac{dp_\infty(y|z)}{dz} \log p_\infty(y|z) \right) + \mathcal{O}\left(\frac{1}{N}\right). \quad (\text{A8})$$

Performing the integral within the sum gives

$$\begin{aligned} \int_0^1 dz \frac{dp_\infty(y|z)}{dz} \log p_\infty(y|z) &= \left[p_\infty(y|z) (\log p_\infty(y|z) - 1) \right]_0^1 \\ &= 0, \end{aligned} \quad (\text{A9})$$

where the second equality follows from $p_\infty(y|0) = p_\infty(y|1)$. Therefore $l_Y(N) \sim \mathcal{O}\left(\frac{1}{N}\right)$ and thus tends to zero in the limit of $N \rightarrow \infty$.
